Applied Physics Letters

RESEARCH ARTICLE | JUNE 06 2023

Broadband transparency of Babinet complementary metamaterials

Special Collection: Fundamentals and Applications of Metamaterials: Breaking the Limits

A. Ospanova ; M. Cojocari ; P. Lamberti ; A. Plyushch ; L. Matekovits ; Yu. Svirko ; P. Kuzhir ; A. Basharin

Appl. Phys. Lett. 122, 231702 (2023)
https://doi.org/10.1063/5.0152841

AIP Publishing

Applied Physics Letters ARTICLE pubs.aip.org/aip/apl

Broadband transparency of Babinet complementary metamaterials

Cite as: Appl. Phys. Lett. **122**, 231702 (2023); doi: 10.1063/5.0152841
Submitted: 2 April 2023 · Accepted: 11 May 2023 ·
Published Online: 6 June 2023

A. Ospanova,[1] M. Cojocari,[1] P. Lamberti,[2] A. Plyushch,[3] L. Matekovits,[4,5,6] Yu. Svirko,[1] P. Kuzhir,[1] and A. Basharin[1,a)]

AFFILIATIONS

[1]Department of Physics and Mathematics, Center for Photonics Sciences, University of Eastern Finland, Joensuu 80101, Finland
[2]Department of Information and Electrical Engineering and Applied Mathematics, University of Salerno, Fisciano 84084, SA, Italy
[3]Faculty of Physics, Vilnius University, Sauletekio 9, Vilnius LT-10222, Lithuania
[4]Department of Electronics and Telecommunications, Politecnico di Torino, Turin 10129, Italy
[5]Department of Measurements and 17 Optical Electronics, Politehnica University Timisoara, Timisoara 300006, Romania
[6]Istituto di Elettronica e di Ingegneria dell'Informazione e delle Telecomunicazioni, National Research Council, Turin 10129, Italy

Note: This paper is part of the APL Special Collection on Fundamentals and Applications of Metamaterials: Breaking the Limits.
[a)]**Author to whom correspondence should be addressed:** alexey.basharin@uef.fi

ABSTRACT

According to the Babinet principle, the diffraction pattern from an opaque body is identical to that from a hole of the same shape and size. Intuitively, placing two complementary structures such as an opaque metal body and its transparent counterpart one by one may result in destructive or constructive interference leading to unexpected electromagnetic response. We propose a Babinet principle-based metamaterial made of two complementary metal/hole checkerboards. The unit cell of each layer is either a metal square with 1/4 of 8 neighboring squares, four of which are made of metal, whereas the other four are square holes, or vice versa. Being placed complementary at optimal distance equal to three-unit cell length, the compound bi-layered Babinet structure demonstrates absolute transparency in a very broad frequency range. The observed absolute transparency of the bi-layered Babinet metasurface is the result of the modified multipole interaction of layers with shifted centers of radiation. We demonstrate both theoretically and experimentally absolute transmission of 0 dB for the Babinet metamaterial made of 3 cm sized Cu squares and complementary holes in the broad frequency range from 4.5 to 6.62 GHz in simulations and from 4.6 to 6.4 GHz in the experiment when the distance between two layers is 1.2 cm. Moving layers toward each other leads to blurring of the resonances. The proven concept of simple, reproducible, and scalable design of the Babinet metamaterial paves the way for the fabrication of broadband transparent devices at any frequency, including THz and optical ranges. The main advantage of broadband Babine metamaterials is applications in optical switching, sensing, filtering, and slow light devices.

The ability to induce transparency of electromagnetic waves and invisibility is a powerful concept that has been a goal of numerous investigations in photonics and metamaterials including effects from cloaking to anapole states.[1] Recently investigated methods to achieve the transparency, such as Fano-resonance,[2–4] classical analog of electromagnetically induced transparency[5–7] (EIT), and anapole states,[8,9] are always based on the interaction of two destructively interfering modes excited in metamolecules. In particular, Fano resonance arises due to the strong interaction of the bright mode, that is the direct interaction of the incident wave with one oscillator, and the dark mode of another oscillator, that is the result of the interaction with near fields of the first oscillator.[2] If resonant frequencies of both oscillators are identical, the EIT effect is associated with symmetrical total transmission peak spectra.[2] Moreover, the anapole state is determined as a system of two multipoles with identical radiation patterns at the same frequency and, depending on engaged particles nature, they are electric anapole,[10,11] magnetic anapole,[12] or hybrid anapole.[13–15] Furthermore, bound states in the continuum (BIC) effect possesses an infinite quality factor originated from trapped modes in scatterers due to the asymmetry of its geometry. On the other hand, all the above effects have a high-quality factor due to narrowband response and find applications as narrowband filters, slow light devices, sensors, and for enhancement of near-fields.

In contrast, in this Letter, we demonstrate a broadband transparency effect in Babinet checkboard complementary metamaterials on

the base of modified multipole approach and perform proof-of-concept experiments in the microwave regime.

Reflection and transmission of electromagnetic waves in metamaterials can be conventionally described by considering secondary waves radiated by currents, which have been induced in the object by the incident wave. In the long wave approximation, when the distance between observation point is much larger than the size of the object, the electric field of the wave at frequency ω generated by current density $j(r)$ is conventionally presented in the following form:[16]

$$\boldsymbol{E}_{rad} = i\omega\mu_0 \int_V \boldsymbol{n} \times [\boldsymbol{j}(r') \times \boldsymbol{n}] \frac{e^{-ikR}}{R} d^3r', \tag{1}$$

where $R = |\boldsymbol{r}' - \boldsymbol{r}|$ is the distance between point r' inside the scattering volume and observation point r, n is a unit vector toward the observation point, V is the medium volume, μ_0 is the vacuum magnetic permeability, and $k = \omega/c$ is the wave number. We consider the normal incidence of the plane wave at a planar metamaterials comprising two thin parallel checkerboards separated by distance $D = 2d$. We assume that the incident wave propagates along the checkerboard normal, which coincides with the z axis of the laboratory Cartesian frame (see Fig. 1).

The reflected and transmitted waves are determined in Eq. (1) at $n = -z$ and $n = +z$, respectively. If the checkerboards comprising the metasurface coincides with $z = \pm d$ planes, Eq. (1) yields for the field at the $z = z_0$ plane,

$$\boldsymbol{E}_{rad} = i\omega\mu_0 \left[\int\int_{S1} \boldsymbol{j}_1(x', y') \frac{e^{ikR_+}}{R_+} dx'dy' + \int\int_{S2} \boldsymbol{j}_2(x', y') \frac{e^{ikR_-}}{R_-} dx'dy' \right], \tag{2}$$

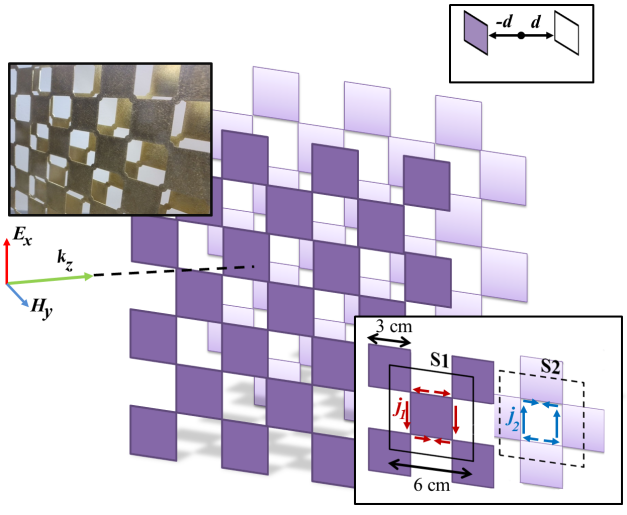

FIG. 1. Babinet metamaterial comprises metallic checkerboard-like surface "S1" and its complementary surface "S2" on the distance $D = 2d$. A normal incidence of plane wave polarized along x axis is assumed. The left inset shows Cu based experimental sample. The top right inset demonstrates the distance of surfaces from the origin of multipole decomposition. Bottom right insertion defines unit cell configuration.

where $j_{1,2}$ are surface densities of the currents flowing in the planes $z = -d$ and $z = +d$, respectively, and $R_\pm = \sqrt{x'^2 + y'^2 + (z_0 \pm d)^2}$.

In the Fraunhofer limit,[17] when the distance to the observation point is much higher than the wavelength and size of the checkerboard unit cell, Eq. (2) can be reduced to the integration over the unit cell. Conventionally, in the long wavelength approximation, the radiated field can be presented in terms of the multipole moments of the metasurface unit cell, which are determined by the current densities $j_\pm$ flowing in each checkerboard. In particular, the radiated field propagating along the direction $n = -z$ describes reflection from the metasurface and can be presented in the following form:[30,31]

$$\boldsymbol{E}_{rad} = \frac{\mu_0 c^2}{2a^2} \Big(ik[\boldsymbol{z} \times [\boldsymbol{P} \times \boldsymbol{z}]] - ik[\boldsymbol{z} \times \boldsymbol{M}] + k^2[\boldsymbol{z} \times (\boldsymbol{z} \times \boldsymbol{Q}^e)] + \frac{k^2}{2}[\boldsymbol{z} \times [\boldsymbol{Q}^m \boldsymbol{z}]] \Big) e^{-ikz_0}, \tag{3}$$

where $\boldsymbol{P}$ is the electric dipole, $\boldsymbol{M}$ is the magnetic dipole, and Q^e is the electric and Q^m is the magnetic quadrupoles. In the Cartesian frame having origin in the center of the unit cell, the multiple moments, which contribute to the radiated field in the frequency range of interest, can be presented in the following form of modified multipoles:[18]

$$\begin{aligned}
\boldsymbol{P} &= \frac{1}{i\omega} \int\int_{S1} \boldsymbol{j}_1 dx'dy' + \frac{1}{i\omega} \int\int_{S2} \boldsymbol{j}_2 dx'dy', \\
\boldsymbol{M} &= \frac{1}{2c} \int\int_{S1} [(\boldsymbol{r}' - \boldsymbol{z}d) \times \boldsymbol{j}_1] dx'dy' + \frac{1}{2c} \int\int_{S2} [(\boldsymbol{r}' + \boldsymbol{z}d) \times \boldsymbol{j}_2] dx'dy', \\
Q^e_{\alpha\beta} &= \frac{1}{2i\omega} \int\int_{S1} \Big[((r'_\beta - d_\beta) j_{1,\alpha} + (r'_\alpha - d_\alpha) j_{1,\beta}) \\
&\quad - \frac{2}{3} \delta_{\alpha,\beta} ((\boldsymbol{r}' - \boldsymbol{d}) \cdot \boldsymbol{j}_1) \Big] dx'dy' \\
&\quad + \frac{1}{2i\omega} \int\int_{S2} \Big[((r'_\beta + d_\beta) j_{2,\alpha} + (r'_\alpha + d_\alpha) j_{2,\beta}) \\
&\quad - \frac{2}{3} \delta_{\alpha,\beta} ((\boldsymbol{r}' + \boldsymbol{d}) \cdot \boldsymbol{j}_2) \Big] dx'dy', \\
Q^m_{\alpha\beta} &= \frac{1}{3c} \int\int_{S1} [(\boldsymbol{r}' - \boldsymbol{d}) \times \boldsymbol{j}_1]_\alpha (\boldsymbol{r}' - \boldsymbol{d})_\beta \\
&\quad + (\boldsymbol{r}' - \boldsymbol{d})_\alpha [(\boldsymbol{r}' - \boldsymbol{d}) \times \boldsymbol{j}_1]_\beta dx'dy' \\
&\quad + \frac{1}{3c} \int\int_{S2} [(\boldsymbol{r}' + \boldsymbol{d}) \times \boldsymbol{j}_2]_\alpha (\boldsymbol{r}' + \boldsymbol{d})_\beta \\
&\quad + (\boldsymbol{r}' + \boldsymbol{d})_\alpha [(\boldsymbol{r}' + \boldsymbol{d}) \times \boldsymbol{j}_2]_\beta dx'dy',
\end{aligned} \tag{4}$$

where the integration of current density j is carried out over the entire volume of the unit-cell and δ is the Kronecker symbol, and $\alpha, \beta = x, y$ or z. S1 and S2 are the area of unit cells of the first and second layer, respectively (Fig. 1). We analyze the definitions for multipoles for layers shifted from the coordinate center and consider it by translation vector $\boldsymbol{d}$.[18] We note, that multipole moments should be calculated relative to the center of mass of the system.[18–20] Higher multipoles do not contribute to the response of our metamaterial and are not included in Eq. (3).

Thus, the full transparency of the metamaterial can be realized contributions from the first and second layers in Eq. (4) compensate each other. In contrast, transparency should be suppressed.

That is in the framework of the multiple decomposition, the radiated field may vanish if the multipole moments originated from the

integrals from the first layer $\boldsymbol{\rho}_1$ and second layer $\boldsymbol{\rho}_2$ compensate one another. For example, if $\boldsymbol{\rho}_1 + \boldsymbol{\rho}_2 = 0$, the dipole mechanism does not contribute to the radiated field and one may expect that reflection will be considerably suppressed. Here, $\boldsymbol{\rho}_1$ and $\boldsymbol{\rho}_2$ are the main intensive multipoles defined response of the system and have opposite phases. However, it is worth noting that if the unit cell size is comparable with the wavelength, the magneto-dipole and quadrupole radiation mechanisms may essentially affect transmission and reflection.

In this sense, two Babinet checkboard complementary layers[29] with opposite directed multipoles can be promising candidates for demonstration of full transparency effect arising due to shifted multipoles excited in different layers.

Indeed, the Babinet principle says that the diffraction pattern from an opaque body is identical to that from a hole of the same shape and size. The textbook[16] example is a narrow slot cut in an infinite plane conducting sheet and linear antenna of the same size. When the slot is illuminated with a normally incident plane wave having the electric field perpendicular to it, the radiation pattern will coincide with that of the with electric field along the antenna. It is worth noting that polarization of the electromagnetic waves scattered by the slot and antenna will be opposite in sign, but of the same amplitude. When we replace them with a square hole and a free-standing square metal sheet of the same size and orientation, the square symmetry implies that orientation of the electric field in scattered waves will be opposite; however, their polarization will be the same. In such a case, one may expect that when two such complementary—in the Babinet sense—objects are irradiated by the same electromagnetic wave, the waves scattered by each object will interfere, i.e., the diffraction pattern will depend on their mutual arrangement. This approach can be extended to a periodic structure, for example, to a pair of complementary parallel checkerboard layers made of the same metal. When the distance between checkerboards is zero, we arrive at a continuous metal sheet. When we shift them with respect to one another, there appears a phase shift between waves scattered by each checkerboard layer. If they are shifted by a distance much smaller than the wavelength, the phase difference between waves scattered by each checkerboard is small and they nearly compensate one another and 100% of the incident radiation will be reflected. However, when shift increases, the interference effects should manifest themselves in the distortion of the diffraction pattern, i.e., it should essentially influence both reflection and transmission. It is worth noting that when the distance between checkerboard layers is comparable with the wavelength, the electromagnetic coupling between them driven by near-field effects will also modify the diffraction pattern providing additional tools to control the transmitted and reflected waves. Recently, the Babinet principle was applied to inverse design of artificial metamaterials based on concave split ring resonators, exhibiting that the complementary split ring resonators (SRR) and c-SRRs demonstrate complementary spectral responses.[21–23] Moreover, complementary metamaterials were used for metalenses applications[24] and dynamically Babinet-invertible meta-filters.[25] Babinet principle formulated for patterns composed of rounded nano-object miniarrays has been discussed in Ref. 26.

In order to demonstrate that bilayer metamaterial allows us to manipulate transmittance spectrum in a wide spectral range, we theoretically and experimentally study the metallic Babinet metamaterial based on the spatially separated two parallel planes having checkerboard-like patterns, which are shifted with respect to one another by half-period (see Fig. 1). That is, if the distance between planes is zero, one arrives at the continuous nontransparent screen.

We perform a simulation of the Babinet metamaterial in the Comsol multiphysics simulator using the Time domain modeling approach with periodic boundary conditions. The period of the unit cell is $a = 6$ cm, the thickness of copper layer is 2 mm, and the distance between screens $D = 2d = 12$ cm. In the result of the simulation, transmission spectra have shown ultra-broadband absolute transmission from 4.5 to 6.62 GHz with 0 dB that is a result of great practical interest (Fig. 2).

Furthermore, we consider interpreting the nature of the transparency effect by multipoles contribution [Eq. (4)]. For this aim, the direct calculation of the Cartesian multipole moments can be obtained via integrating the induced density of displacement currents j over the whole volume of the unit cell, as depicted in the inset of Fig. 1. Here, we consider the monochromatic time dependence in the view of $e^{i\omega t}$. The multipole moments are considered in terms of dipoles and quadrupoles of electric and magnetic nature that is more intensive among all multipoles in the system, by using Eq. (4). For clarity, let us consider the intensity of multipoles separately for the case of first layer "*S*1" in the coupled system of second layer "*S*2" [Fig. 3(a)], the case of second layer *S*2 in the coupled system of first layer *S*1 [Fig. 3(b)], as well as the case of irradiation from the system of both coupled layers

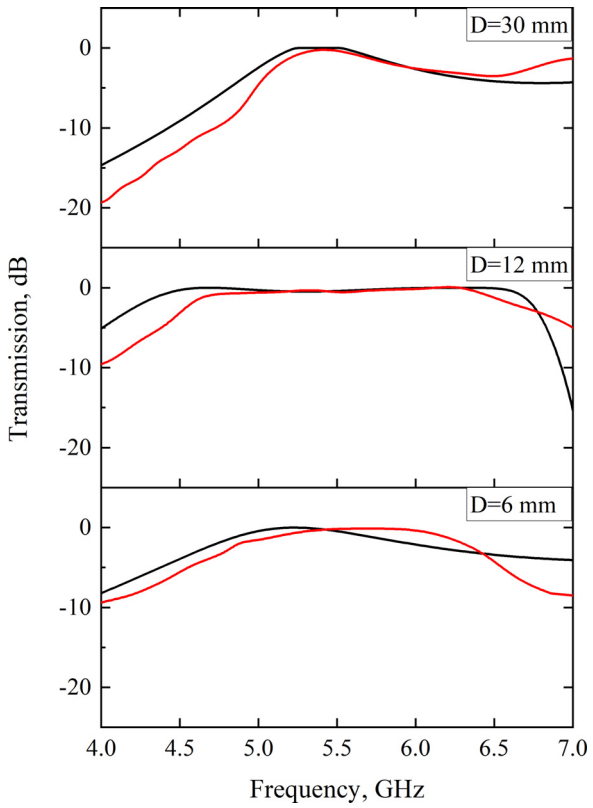

FIG. 2. Simulated and measured transmission spectra (S21) dependence on frequency (black curve, Comsol Multiphysics) and measured (red curve) spectra for different distances $D = 6$, 12, and 30 mm.

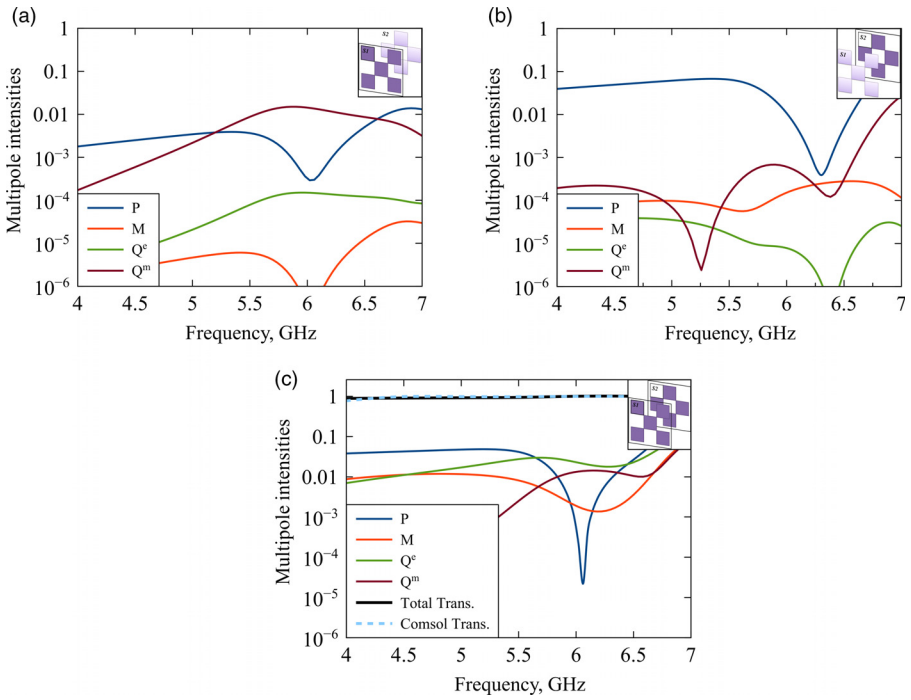

FIG. 3. Simulated multipoles intensity in terms of dipoles and quadrupoles of electric and magnetic origin in 4–7 GHz frequency range. Here, **P** stands for electric dipole moment, **M** stands for magnetic dipole moment; $\mathbf{Q}^{\mathbf{e}}$ and $\mathbf{Q}^{\mathbf{m}}$ stand for quadrupoles of electric and magnetic origin, respectively. (a) The intensity of multipoles separately for the case of first layer "S1" in the coupled system of second layer "S2," (b) the case of second layer "S2" in the coupled system of first layer "S1," and (c) the case of irradiation from the system of both coupled layers.

*S*1, *S*2 [Fig. 3(c)], by taking into account the shift d of each layer relative to coordinate origin by using Eq. (4).

The origin of the strongly pronounced wide peak at 4–6.5 GHz (Fig. 2) cannot be explained directly by multipoles contribution of whole metamaterial, Fig. 3(c). Comprehension of the effect may be obtained only by using modified multipoles and by method of secondary multipole analysis.[18,19,27,28] We can present every multipole moment of metamaterial as a sum of the same order multipole moments of the layer (the layer *S*1 and layer *S*2) calculated with respect to the same center of mass. For this aim, we consider the current densities of each layer separately (but in the case of irradiation of the whole system), Eq. (4). For the case of multipoles of the first layer *S*1 within the resonance frequency band 5–6.5 GHz, the transmission is mostly defined by magnetic quadrupole, while dipole irradiation is resonantly suppressed [Fig. 3(a)] and defined by the electric dipole moment beyond resonance. In the case of second layer *S*2 multipole radiation of quadrupoles as well as electric dipole moment is resonantly suppressed, Fig. 3(b). Therefore, in the system of both screens *S*1 and *S*2, we observe that overall radiation from multipoles is suppressed down to 100 times whereas the multipole interaction is also differing, Fig. 3(c). The resonant transmission behavior is underpinned by resonant suppression of electric dipole moment with a smooth intensity of other suppressed multipoles for frequencies within the 5.5–6.5 GHz band and defined by electric dipole moment beyond this resonance. According to these figures, we may conclude that resulting transparency effect occurs due to interaction between multipoles from both screens that also leads to a decrease in overall intensity. It is worth noting that in the case of combination of screens, the total transmission are defined as a sum of multipoles of each screen, Fig. 3(c). The reason for this destructive interaction between multipoles of metamaterial is oppositely directed currents in each layer forming multipoles that are mutually compensated. We also plot total transmission Fig. 3(c) calculated as a sum of multipoles (total trans. curve) and compared it with transmission obtained directly in Comsol Multiphysics simulation (Comsol Trans.), Fig. 3(c). The curves coincide with each other, which confirm that our choice of multipoles families up to quadrupoles is enough and correct.

In order to identify the origin of the broadband peak, we calculated the transmittance of the metamaterials by gradually increasing the distance from $D = 0$ mm up to $D = 30$ mm (Fig. 4). As we already negotiated, each layer determined by its own set of multipoles that corresponds to particular resonances in transmission, which depends on the interlayer distance. The overlap of both complementary layers leads to 0 dB transmission (Fig. 4). Gradually increase in the distance between surfaces ($D = 0.002$ mm) results in the appearance of two main intensive multipole resonances in system ρ_1 and ρ_2 with opposite phases that govern transmission spectrum. Further separation of the surfaces corresponds to the shift of resonance ρ_1 toward another ρ_2 until there is total transmission at the distance $D = 12$ mm. One can observe from Fig. 4 that there appears a gap in the transmittance spectrum in the vicinity of 6 GHz when the distance between layers is $D = 30$ mm.

To prove our concept and observe experimentally the total transparency effect, we fabricated the microwave Babinet metamaterial sample. The experimental specimen was fabricated from copper sheets and their pattern was cut out by laser cutting method. The parameters of the sample are the same as for the simulation model. Obviously, then it can be rescaled up to higher frequencies.

We use an anechoic chamber with dimensions equipped by ECCOSORB absorbers and two wideband horn antennas. S21 parameters (transmission spectra) were measured by two horn antennas method. Two broadband horn antennas for electromagnetic radiation

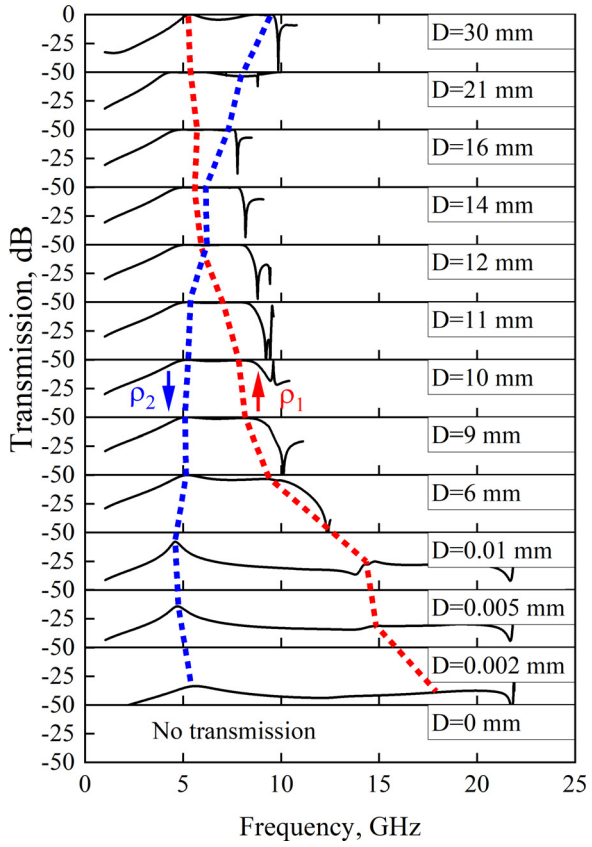

FIG. 4. The evaluation of transmission spectra dependence on distance between layers *D*. Dashed lines indicate the sign of main intensive multipoles ρ_1 and ρ_2 on the distance between them.

and detection were located at a distance 5 m one from the other; the metamaterial sample has been located at the midway between the two horns. In particular a tinfoil-covered plywood screen with a 40×49 cm^2 in it has been used. The transmission spectra of the electromagnetic waves through the metamaterial sample were measured by a Rohde and Schwarz SVB20 vector network analyzer. Measurements have been carried out in the 4–7 GHz frequency band. Measured transmission spectra were compared with simulated data, Fig. 2, and the same result of total transmission was revealed. Moreover, we measured transmission spectra for $D = 6$, 12, and 30 mm in order to evaluate the changing of broad resonance with the distance between layers.

In conclusion, we presented Babinet principle based metamaterial exhibiting ultra-broadband absolute transmission in the 4.5–6.62 GHz band in simulations and the 4.6–6.4 GHz in experiment frequency ranges. The aim of this study is twofold. First of all, we demonstrated the sustainability of modified multipole decomposition as a reliable tool for electrodynamic analysis of structures with shifted multipole centers. Second, we demonstrated ultra-broadband absolute transmission with 0 dB that itself is an advantage for photonics, especially in the case of high-sensitive sensors, broadband filters and others. Broadband transmission are always associated with destructive interference between multipoles leading to suppressing of far-field irradiation and enhancing of the near field irradiation between layers. Thus, placing any scatterer between the layers leads to an increase in transmission or vice versa suppression depending on whether the object is placed in the antinode or in the field maximum. Such a misconfiguration of the multipoles will lead to ultra nearband spectral features in the transmission spectrum of the metamaterial. Regarding the comparison between the anapole concept and method of total transmission presented in this paper, one can state that they are the same from the point of view of suppression of radiating losses. However, the anapole mode is result of destructive interference between electric and toroidal multipole moments excited in the same particle. Here, we present an alternative approach to anapole mode, where the radiating losses are compensated due to destructive interference between any multipoles excited in two different layers of metamaterial. In case the unit cell is extended to incorporate 2D pieces from the two surfaces, the compensation mechanism can be seen as corresponding to the anapole concept.

This effect is provided by such a simple design that in advantage and can be easily reproduced in more appreciated THz and optical frequency range.

This work was supported by the Academy of Finland via Flagship Programme Photonics Research and Innovation (PREIN), Decision No. 320166, and Grant No. 343393, the Horizon 2020 RISE DiSeTCom Project via No. 823728, the Horizon 2020 RISE CHARTIST Project via No. 101007896, the Horizon 2020 RISE TERASSE Project via No. 823878. The authors would like to thank to Mr. Gianluca Dassano from Politecnico di Torino for his help in setting up the measurement system.

AUTHOR DECLARATIONS

Conflict of Interest

The authors have no conflicts to disclose.

Author Contributions

Anar Ospanova: Conceptualization (equal); Investigation (equal); Methodology (equal); Validation (equal); Writing – original draft (equal); Writing – review & editing (equal). **Maria Cojocari:** Investigation (equal). **Patrizia Lamberti:** Investigation (equal); Writing – original draft (equal); Writing – review & editing (equal). **Artyom Plyushch:** Investigation (equal). **Ladislau Matekovits:** Investigation (equal); Methodology (equal); Resources (equal); Validation (equal); Writing – original draft (equal); Writing – review & editing (equal). **Yuri Svirko:** Investigation (equal); Supervision (equal); Writing – original draft (equal); Writing – review & editing (equal). **Polina P. Kuzhir:** Funding acquisition (equal); Investigation (equal); Project administration (equal); Supervision (equal); Validation (equal); Writing – original draft (equal); Writing – review & editing (equal). **Alexey Andreevich Basharin:** Conceptualization (equal); Data curation (equal); Investigation (equal); Methodology (equal); Supervision (equal); Validation (equal); Writing – original draft (equal); Writing – review & editing (equal).

DATA AVAILABILITY

The data that support the findings of this study are available from the corresponding author upon reasonable request.

REFERENCES

[1]G. Labate, A. Alù, and L. Matekovits, "Surface-admittance equivalence principle for nonradiating and cloaking problems," Phys. Rev. A **95**, 063841 (2017).
[2]M. F. Limonov, M. V. Rybin, A. N. Poddubny, and Y. S. Kivshar, "Fano resonances in photonics," Nat. Photonics **11**, 543–554 (2017).
[3]B. Luk'yanchuk, N. I. Zheludev, S. A. Maier, N. J. Halas, P. Nordlander, H. Giessen, and C. T. Chong, "The Fano resonance in plasmonic nanostructures and metamaterials," Nat. Mater. **9**, 707–715 (2010).
[4]A. E. Miroshnichenko, S. Flach, and Y. S. Kivshar, "Fano resonances in nanoscale structures," Rev. Mod. Phys. **82**, 2257 (2010).
[5]S. Zhang, D. A. Genov, Y. Wang, M. Liu, and X. Zhang, "Plasmon-induced transparency in metamaterials," Phys. Rev. Lett. **101**, 047401 (2008).
[6]P. Tassin, L. Zhang, T. Koschny, E. Economou, and C. M. Soukoulis, "Low-loss metamaterials based on classical electromagnetically induced transparency," Phys. Rev. Lett. **102**, 053901 (2009).
[7]N. Papasimakis, V. A. Fedotov, N. Zheludev, and S. Prosvirnin, "Metamaterial analog of electromagnetically induced transparency," Phys. Rev. Lett. **101**, 253903 (2008).
[8]R. M. Saadabad, L. Huang, A. B. Evlyukhin, and A. E. Miroshnichenko, "Multifaceted anapole: From physics to applications," Opt. Mater. Express **12**, 1817–1837 (2022).
[9]K. V. Baryshnikova, D. A. Smirnova, B. S. Luk'yanchuk, and Y. S. Kivshar, "Optical anapoles: Concepts and applications," Adv. Opt. Mater. **7**, 1801350 (2019).
[10]V. A. Fedotov, A. Rogacheva, V. Savinov, D. P. Tsai, and N. I. Zheludev, "Resonant transparency and non-trivial non-radiating excitations in toroidal metamaterials," Sci. Rep. **3**, 2967 (2013).
[11]A. E. Miroshnichenko, A. B. Evlyukhin, Y. F. Yu, R. M. Bakker, A. Chipouline, A. I. Kuznetsov, B. Luk-yanchuk, B. N. Chichkov, and Y. S. Kivshar, "Nonradiating anapole modes in dielectric nanoparticles," Nat. Commun. **6**, 8069 (2015).
[12]P. Kapitanova, E. Zanganeh, N. Pavlov, M. Song, P. Belov, A. Evlyukhin, and A. Miroshnichenko, "Seeing the unseen: Experimental observation of magnetic anapole state inside a high-index dielectric particle," Ann. Phys. **532**, 2000293 (2020).
[13]A. K. Ospanova, A. Basharin, A. E. Miroshnichenko, and B. Luk-yanchuk, "Generalized hybrid anapole modes in all-dielectric ellipsoid particles," Opt. Mater. Express **11**, 23–34 (2021).
[14]B. Luk'yanchuk, R. Paniagua-Domínguez, A. I. Kuznetsov, A. E. Miroshnichenko, and Y. S. Kivshar, "Hybrid anapole modes of high-index dielectric nanoparticles," Phys. Rev. A **95**, 063820 (2017).
[15]A. Canós Valero, E. A. Gurvitz, F. A. Benimetskiy, D. A. Pidgayko, A. Samusev, A. B. Evlyukhin, V. Bobrovs, D. Redka, M. I. Tribelsky, M. Rahmani *et al.*, "Theory, observation, and ultrafast response of the hybrid anapole regime in light scattering," Laser Photonics Rev. **15**, 2100114 (2021).
[16]J. D. Jackson, *Classical Electrodynamics*, 3rd ed. (Wiley, New York, 1999), p. 98.
[17]M. Born and E. Wolf, *Principles of Optics: Electromagnetic Theory of Propagation, Interference and Diffraction of Light* (Elsevier, 2013).
[18]A. Ospanova, M. Cojocari, and A. Basharin, "Modified multipoles in photonics," Phys. Rev. B **107**, 035156 (2023).
[19]V. R. Tuz, V. Dmitriev, and A. B. Evlyukhin, "Antitoroidic and toroidic orders in all-dielectric metasurfaces for optical near-field manipulation," ACS Appl. Nano Mater. **3**, 11315–11325 (2020).
[20]R. E. Raab and O. L. De Lange, *Multipole Theory in Electromagnetism: Classical, Quantum, and Symmetry Aspects, with Applications* (OUP, Oxford, 2004), Vol. 128.
[21]F. Falcone, T. Lopetegi, M. Laso, J. Baena, J. Bonache, M. Beruete, R. Marqués, F. Martín, and M. Sorolla, "Babinet principle applied to the design of metasurfaces and metamaterials," Phys. Rev. Lett. **93**, 197401 (2004).
[22]C. Rockstuhl, T. Zentgraf, T. P. Meyrath, H. Giessen, and F. Lederer, "Resonances in complementary metamaterials and nanoapertures," Opt. Express **16**, 2080–2090 (2008).
[23]L. Zhang, T. Koschny, and C. M. Soukoulis, "Creating double negative index materials using the Babinet principle with one metasurface," Phys. Rev. B **87**, 045101 (2013).
[24]X. Ni, S. Ishii, A. V. Kildishev, and V. M. Shalaev, "Ultra-thin, planar, Babinet-inverted plasmonic metalenses," Light: Sci. Appl. **2**, e72 (2013).
[25]Y. Urade, Y. Nakata, K. Okimura, T. Nakanishi, F. Miyamaru, M. W. Takeda, and M. Kitano, "Dynamically Babinet-invertible metasurface: A capacitive-inductive reconfigurable filter for terahertz waves using vanadium-dioxide metal-insulator transition," Opt. Express **24**, 4405–4410 (2016).
[26]E. Tóth, B. Bánhelyi, O. Fekete, and M. Csete, "Metamaterial properties of Babinet complementary complex structures," Sci. Rep. **13**, 4701 (2023).
[27]A. A. Basharin, E. Zanganeh, A. K. Ospanova, P. Kapitanova, and A. B. Evlyukhin, "Selective superinvisibility effect via compound anapole," Phys. Rev. B **107**, 155104 (2023).
[28]A. K. Ospanova, A. Karabchevsky, and A. A. Basharin, "Metamaterial engineered transparency due to the nullifying of multipole moments," Opt. Lett. **43**, 503–506 (2018).
[29]K. Kempa, "Percolation effects in the checkerboard Babinet series of metamaterial structures," Phys. Status Solidi (RRL) **4**, 218–220 (2010).
[30]V. Savinov, V. A. Fedotov, and N. I. Zheludev, "Toroidal dipolar excitation and macroscopic electromagnetic properties of metamaterials," Phys. Rev. B **89**, 205112 (2014).
[31]P. D. Terekhov, V. E. Babicheva, K. V. Baryshnikova, A. S. Shalin, A. Karabchevsky, and A. B. Evlyukhin, "Multipole analysis of dielectric metasurfaces composed of nonspherical nanoparticles and lattice invisibility effect," Phys. Rev. B **99**, 045424 (2019).